Available online at www.sciencedirect.com
SCIENCE DIRECT®
Journal of Molecular Spectroscopy 236 (2006) 127–133
Journal of MOLECULAR SPECTROSCOPY
www.elsevier.com/locate/jms

Fourier-transform absorption spectroscopy of $H_2{}^{18}O$ in the first hexade region

A.-W. Liu [a,b], O. Naumenko [b,c], K.-F. Song [a], B. Voronin [c,d], S.-M. Hu [a,b,*]

[a] Hefei National Laboratory for Physical Sciences at Microscale, University of Science and Technology of China, Hefei 230026, China
[b] Shanghai Institute for Advanced Studies, University of Science and Technology of China, Shanghai 201315, China
[c] Institute of Atmospheric Optics, SB, Russian Academy of Science, Tomsk, Russia
[d] Department of Physics and Astronomy, University College London, London WC1E 6BT, UK

Received 27 December 2005

Abstract

The Fourier-transform absorption spectrum of $H_2{}^{18}O$ was recorded in the 6000–7940 cm^{-1} region and assigned on the base of the very accurate ab initio calculations by Partridge and Schwenke (PS) [J. Chem. Phys. 106 (1997) 4618–4639; J. Chem. Phys. 113 (2000) 6592–6597]. A set of 821 accurate rovibrational energy levels was obtained for six interacting states of the first hexad: (101), (120), (021), (200), (002), and (040). 290 of them are reported for the first time. The experimental line intensities are also estimated and compared with the PS calculations and the available literature data in the considered spectral range.

Keywords: Vibration–rotation spectroscopy; Water vapor absorption; Spectroscopic parameters

1. Introduction

As the second primary isotope of the water molecule, $H_2{}^{18}O$ and its infrared absorption contributes noticeably to the atmospheric absorption and should be taken into account in the explanation of atmospheric radiation balance.

The spectrum under present study is formed by transitions coming on the first hexad upper vibrational states: (101), (200), (002), (120), (021), and (040), it occupies 6000–7940 cm^{-1} spectral region and has been investigated, since 1986 in a number of papers [1–5]. Chevillard et al. [1] presented first consistent study of the first hexad energy levels and line intensities. Toth [2] reported $H_2{}^{18}O$ and $H_2{}^{17}O$ transitions frequencies and strengths from 6600 to 7640 cm^{-1}. $H_2{}^{18}O$ absorption spectra are also considered in some very recent contributions. Macko et al. [3] recorded the pure water absorption spectrum in the 6130–6749 cm^{-1} region by means of the high sensitive CRDS technique. An important set of 139 new energy levels was derived from very weak transitions of $H_2{}^{18}O$ present in the sample in natural abundance. Tolchenov et al. [4] retrieved weak pure water vapor transitions in the 7400–9600 cm^{-1} region from a long path length FT spectrum. In their work, among more than 1000 lines recorded in the region overlapping with present study, 108 lines were assigned to $H_2{}^{18}O$ transitions reaching the (101), (200), and (002) stretching states. Toth [5] also updated his earlier results on water and its main isotope species absorption in the 500–7782 cm^{-1} region. All these results were collected and validated in a database on the energy levels, transitions frequencies and strengths of $H_2{}^{18}O$ [6].

Despite all the above mentioned works, the high resolution study of $H_2{}^{18}O$ in the 6000–8000 cm^{-1} region is not yet completed, compared with detailed simulation by Partridge and Schwenke (PS) [7,8]. Many lines predicted with relatively strong and middle intensities are not yet observed. In this case, we present here the high resolution

* Corresponding author. Fax: +86 551 3602969.
E-mail address: smhu@ustc.edu.cn (S.-M. Hu).

0022-2852/$ - see front matter © 2006 Elsevier Inc. All rights reserved.
doi:10.1016/j.jms.2006.01.003

Fourier-transform study of the $H_2{}^{18}O$ absorption spectrum in the above region.

2. Experimental details

The ^{18}O enriched water sample was purchased from Aldrich Chemical Company, Inc. The stated isotopic concentration of ^{18}O is 95%. The absorption spectra were recorded with a Bruker IFS 120HR Fourier-transform spectrometer equipped with a path length adjustable multi-pass gas cell. A tungsten source, CaF_2 beam splitter, and Ge-diode detector were used. The cell was operated at room temperature (297 ± 1 K), stabilized by an air-conditioning system. The pressure was measured using two capacitance manometers of 200 Pa and 133 hPa full-scale range with an overall accuracy of 0.5%. Because of the large variation of the line intensities in this spectral region, four measurements were carried out with different sample pressure and absorption path lengths. They are: (1) 11 Pa, 15 m, (2) 215 Pa, 15 m, (3) 1307 Pa, 15 m, and (4) 1307 Pa, 105 m. The line positions were calibrated with water lines given by the HITRAN-2004 [9] database. The accuracy of the line positions of unblended and not-very-weak lines was estimated to be better than 0.0012 cm^{-1}. A portion of the spectrum is presented in Fig. 1.

Because, we could not substitute all the water molecules adsorbed on the walls of the cell with the limited amount of sample, it is difficult to accurately determine the real isotope concentration of $H_2{}^{18}O$ in our measurements. For the purpose to compare the experimental line intensities with HITRAN-2004 [9] and PS predictions, approximate experimental intensities were derived as follow: first, we retrieved the integrated absorbance of some well isolated $H_2{}^{18}O$ lines with 5–50% absorption depths in each spectrum from line profile fitting, then the relative ratio of the absorbance of the same line was used to scale all the other line intensities from each spectrum. In this case, all the relative line intensities were retrieved and they were further scaled against the spectrum recorded at 1307 Pa and 15 m. Then, the isotopic abundance of the 1307 Pa sample was estimated by comparing the experimental line intensities of some moderate lines with the values given in [2]. In this way, we could estimate the $H_2{}^{18}O$ abundance was 75% in the measurement at 1307 Pa and 15 m. So, approximate line intensities can be obtained for each line. We estimate the precision of the values of well isolated and not-very-weak lines is about 10%.

3. Results and discussion

3.1. Experimental linelist construction and identification

The experimental linelist together with the PS simulated spectrum are used as the input data for the program for automatic rovibrational spectra assignment. At the first stage of spectrum assignment, we kept in the experimental list all the recorded lines among which there were absorption lines belonging to all the isotope species other than $H_2{}^{18}O$ like $H_2{}^{16}O$, $H_2{}^{17}O$, and $HD^{18}O$ present in the sample. The reason for this is, first, that many $H_2{}^{18}O$ lines overlap with the absorption features of other isotopes; second, it is difficult to discriminate the $HD^{18}O$ lines. When the strong part of $H_2{}^{18}O$ spectrum was identified, we have cleaned the spectrum from pure $H_2{}^{17}O$ and $H_2{}^{16}O$ lines by comparison with [1,2,4] data and performed final identification list where only assigned $H_2{}^{18}O$ lines were included.

The quality of the PS prediction is found to be very high that the obs. – calc. deviations of line positions do not exceed 0.36 cm^{-1}. In average, the deviation is only about

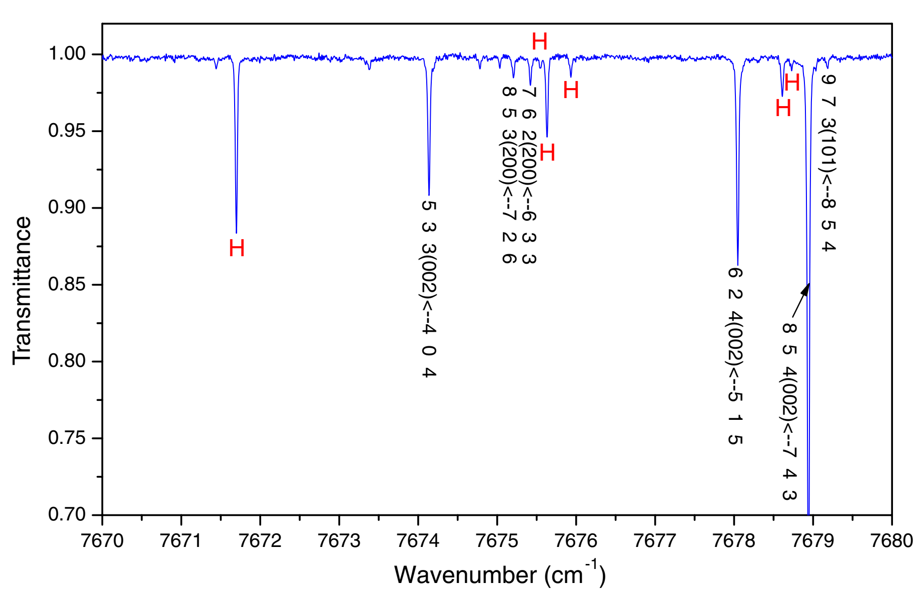

Fig. 1. The spectrum in the 7670–7680 cm^{-1} region recorded with 0.015 cm^{-1} unapodized resolution. Sample gas pressure 1307 Pa; absorption path length 105 m. $H_2{}^{16}O$ lines are marked with ‘H’.

$0.05\ cm^{-1}$. Matching between observed and calculated intensities, which is one of the main criteria in the assignment process, was quite satisfactory and provided unambiguous identification. In this case, the spectrum assignment would be straightforward, but for high density of the spectral lines and the presence of several isotope species. In some cases, it was difficult to select true experimental line from several possibilities for one predicted line. Certain cautions were also taken in attaching several identifications (if needed) to the same experimental line.

The final identification list of the $H_2{}^{18}O$ molecule in the 6000–7940 cm^{-1} region is attached to this paper as Supplementary material. This list contains 2955 absorption lines which correspond to 3168 transitions taking into account all components of the blended lines. For each line, the experimental and calculated PS intensities are given followed by rovibrational assignment. Lines superimposed to $H_2{}^{16}O$ and $H_2{}^{17}O$ are specially marked. The identification list contains also 187 hot transitions originating from the (010) state and involving the second hexad upper states. Part of the $H_2{}^{18}O$ lines was unrecoverable superimposed to stronger $H_2{}^{16}O$ lines in their vicinity, and thus was not included into the resulting linelist.

It turns out that the HITRAN-2004 [9] database contains only 1286 $H_2{}^{18}O$ lines in the same spectral region as considered here. It is also interesting to compare our experimental line intensities with the calculated PS values and those from the HITRAN database. They are shown in Fig. 2 for 100% $H_2{}^{18}O$ isotope abundance. Though we evidence a number of considerable disagreements in intensities, as it is clearly seen in the figure, the averaged intensity ratio $I_{\text{this work}}/I_{\text{PS}}$, $I_{\text{this work}}/I_{\text{HITRAN}}$ in two panels for all the lines in common with this work was found to be close to 1.0. It indicates a good quality both of the PS calculation and our experimental intensity estimation, and confirms as well our assignments. Some examples of the largest disagreement between our and HITRAN-2004 data can be found in the Supplementary materials to this paper. The list contains 64 $H_2{}^{18}O$ absorption lines from the HITRAN database followed by comparison with our data. Thirty-three of them are not confirmed in this work, since they either deviated in strength up to 1000 times from the PS calculation and our intensity estimation or were misassigned.

3.2. Energy levels derivation

The set of 821 energy levels is derived from the assigned transitions by adding the ground state energy levels [10].

Table 1
Summary of the obtained experimental information

VIB	E_v (cm^{-1})	Number of levels			
		This work	Ref. [6]	In common	New
040	6110.41	78	63	58	20
120	6755.510	123	88	83	40
021	6844.598	146	111	110	36
200	7185.877	152	107	101	51
101	7228.877	179	122	118	61
002	7418.724	143	66	61	82
Total		821	557	531	290

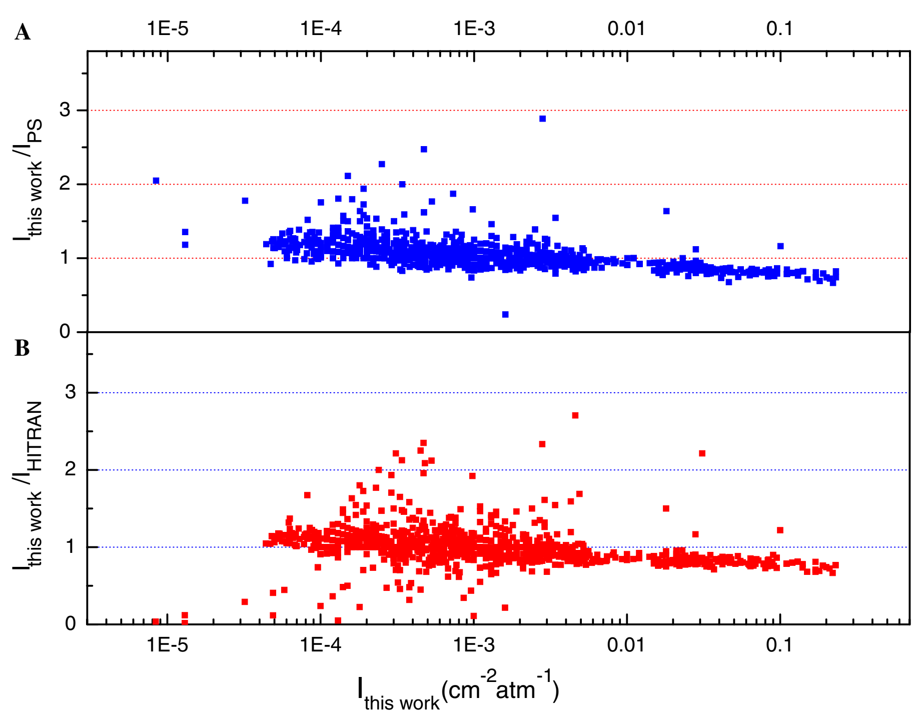

Fig. 2. Comparison of the line intensities for pure $H_2{}^{18}O$ from this work with those given by HITRAN-2004 database and predicted by Schwenke and Partridge [8].

Table 2
Rovibrational energy levels (in cm^{-1}) of $H_2{}^{18}O$ in the studied region

V	*J*	K_a	K_c	*E*	δ	*N*
101	7	7	0	8524.0091	0.4	2
101	8	7	2	8712.8614		1
101	8	8	1	8901.8238	2.1	3
101	8	8	0	8901.8256	1.3	3
101	9	5	4	8632.1758	0.6	4
101	9	7	3	8925.5510	0.1	2
101	9	7	2	8925.5118	0.6	2
101	9	8	2	9119.7866	0.2	3
101	9	8	1	9119.7867	0.3	3
101	9	9	1	9270.6304	0.8	2
101	9	9	0	9270.6296	2.2	2
101	10	4	7	8741.9649	0.7	2
101	10	5	6	8866.1028	0.1	3
101	10	6	5	9003.8519	3.5	2
101	10	7	4	9161.9447	0.6	3
101	10	7	3	9161.8083	2.5	2
101	10	8	3	9360.4948		1
101	10	8	2	9360.4712	0.3	3
101	10	9	2	9507.8183		1
101	10	9	1	9507.8205	1.9	2
101	11	3	8	8981.3578	0.6	3
101	11	4	8	8994.9499	0.7	3
101	11	5	7	9125.3454	0.7	3
101	11	5	6	9143.0059	0.3	3
101	11	6	6	9264.4455	0.1	2
101	11	6	5	9265.7087	0.2	3
101	11	7	5	9421.9544	1.0	2
101	11	7	4	9421.6161		1
101	11	8	3	9623.9320		1
101	11	9	3	9768.1566	8.8	2
101	11	9	2	9768.1478		1
101	12	2	10	9112.9092	0.6	4
101	12	3	10	9112.9891	1.5	3
101	12	4	9	9267.1901	0.7	3
101	12	4	8	9376.6366	0.4	3
101	12	5	8	9406.0466	0.4	2
101	12	5	7	9437.6473	1.5	2
101	12	6	7	9547.9826	6.4	2
101	12	6	6	9552.1217	0.0	2
101	12	7	6	9705.4581		1
101	13	0	13	8965.1884		1
101	13	1	12	9190.0755	0.2	3
101	13	2	12	9190.0205	0.8	3
101	13	2	11	9386.7645	0.6	2
101	13	3	11	9387.5597	0.2	2
101	13	3	10	9557.9771	1.0	2
101	13	4	10	9557.7187	0.5	3
101	13	4	9	9683.9855	0.1	2
101	13	5	9	9707.2583	0.7	3
101	13	6	8	9853.7119	3.8	2
101	13	6	7	9863.7177		1
101	14	0	14	9221.6853	0.1	2
101	14	1	14	9221.6852	0.3	2
101	14	2	12	9678.6088		1
101	14	3	11	9862.8179		1
101	14	4	10	10012.3490		1
101	14	5	9	10105.8269		1
101	15	0	15	9495.4183	0.1	2
101	15	2	14	9755.8766		1
101	15	3	13	9987.1773		1
101	16	0	16	9786.3037	1.6	2
101	16	1	16	9786.3034	1.4	2
101	16	1	15	10064.3759		1
101	18	0	18	10419.1862		1
101	18	1	18	10419.1862		1
021	6	6	1	8023.3783	1.5	3
021	7	7	1	8405.4037	0.4	2
021	7	7	0	8405.4057	1.4	2
021	8	6	3	8387.8510	0.6	2
021	8	6	2	8387.8783	0.6	3
021	8	7	2	8600.3079	2.0	2
021	8	7	1	8600.3105	0.8	3
021	8	8	1	8827.8575	0.2	2
021	8	8	0	8827.8575	0.0	2
021	9	5	4	8416.2674	0.3	3
021	9	6	3	8605.9815	0.2	2
021	9	7	3	8818.8219	0.4	2
021	9	7	2	8818.8217	3.9	3
021	9	8	2	9046.8385	0.6	2
021	9	8	1	9046.8389	0.7	2
021	10	5	6	8656.6559	0.6	2
021	10	5	5	8660.2081	0.6	4
021	10	7	4	9060.7071		1
021	10	7	3	9060.7264		1
021	10	8	3	9288.8184		1
021	10	8	2	9288.8193		1
021	11	2	9	8564.1251	0.1	3
021	11	3	9	8573.6151	0.3	3
021	11	3	8	8698.7020	0.2	2
021	11	4	7	8795.7785	1.3	3
021	11	5	7	8921.2484	1.6	2
021	11	5	6	8929.6952		1
021	11	6	6	9112.6362		1
021	11	6	5	9113.7325	3.6	2
021	11	7	5	9325.7279	0.4	2
021	12	1	12	8358.2202	0.7	2
021	12	2	11	8620.0250	4.3	3
021	12	2	10	8834.4588	0.2	2
021	12	3	10	8839.6522	0.9	2
021	12	3	9	8992.8159		1
021	12	4	9	9028.5665		1
021	12	4	8	9099.8647		1
021	12	5	7	9227.9375		1
021	12	6	6	9403.6089		1
021	13	1	13	8598.2299	0.1	2
021	13	2	12	8883.2973	0.7	2
021	13	3	11	9123.3816	0.1	2
120	5	4	2	7447.4427	0.2	2
120	5	5	1	7619.7895	0.1	2
120	6	6	0	7964.3813		1
120	7	3	5	7614.2624	0.1	3
120	7	5	3	7932.8101	0.6	3
120	7	5	2	7932.9488	0.5	2
120	7	6	2	8133.4532		1
120	7	6	1	8133.4492	3.4	2
120	7	7	1	8357.4673	0.0	2
120	7	7	0	8357.4672	0.3	2
120	8	5	3	8125.6521	0.2	3
120	8	6	3	8326.3584	0.2	2
120	8	6	2	8326.3785		1
120	8	8	1	8795.7981		1
120	8	8	0	8795.7959		1
120	9	1	8	7841.5486	0.2	3
120	9	3	7	8011.6498		1
120	9	3	6	8071.1116		1

Only NEW energy levels are presented here. A full list is given in Supplementary material. *N* is the number of transitions used for the upper level determination and δ denotes the corresponding experimental uncertainties in 10^{-3} cm^{-1}.

Table 2 (*continued*)

V	J	K_a	K_c	E	δ	N
120	9	5	5	8340.6908	1.8	2
120	9	7	3	8768.9464	1.1	2
120	9	7	2	8768.9437	0.7	2
120	9	9	1	9317.7478		1
120	9	9	0	9317.7480		1
120	10	1	9	8053.3388	1.0	2
120	10	2	9	8056.1748	0.6	3
120	10	2	8	8217.1172		1
120	10	3	8	8243.3347	0.9	3
120	10	3	7	8325.9803	0.8	2
120	10	4	7	8401.0279	0.0	2
120	10	4	6	8428.9026		1
120	10	5	6	8582.7111		1
120	10	5	5	8584.0552		1
120	10	7	4	9009.3990	2.6	2
120	10	7	3	9009.3954		1
120	11	1	10	8282.0530	0.5	4
120	11	2	9	8472.4308	0.3	2
120	11	3	9	8477.6680		1
120	11	3	8	8602.4773	0.9	3
120	11	4	7	8704.7428	0.6	2
120	11	7	5	9272.9428		1
120	11	7	4	9272.9543		1
120	12	0	12	8264.6749	0.7	2
120	12	1	12	8259.1043	0.1	2
120	12	3	10	8745.0614		1
120	12	4	9	8940.5571	0.3	2
120	12	5	8	9131.0440		1
120	13	0	13	8499.5123		1
120	13	3	10	9212.2741		1
200	7	7	1	8497.8590	0.7	2
200	8	3	5	8197.9076	0.7	3
200	8	4	4	8270.4823	0.7	4
200	8	5	4	8378.7444	0.4	6
200	8	5	3	8381.8039	0.6	5
200	8	6	3	8524.0707	0.5	4
200	8	7	1	8688.2983	1.8	2
200	8	8	1	8874.0646	0.2	2
200	8	8	0	8874.0644	0.4	2
200	9	1	9	8067.9423	0.5	3
200	9	3	6	8422.9636	0.3	3
200	9	5	5	8597.2832	0.5	6
200	9	5	4	8597.0958	0.6	3
200	9	7	3	8902.1120		1
200	9	7	2	8902.1260	0.3	3
200	9	8	2	9089.4114	0.3	2
200	9	9	1	9261.8044		1
200	9	9	0	9261.8046		1
200	10	2	8	8567.8869	0.3	3
200	10	3	7	8670.5258	1.2	3
200	10	4	6	8741.9342	0.5	2
200	10	5	6	8833.3279	0.2	4
200	10	5	5	8837.8858	0.2	3
200	10	7	4	9139.1748	0.5	3
200	10	7	3	9139.2431		1
200	10	8	2	9327.9898		1
200	11	0	11	8457.5329	0.4	4
200	11	1	11	8457.6596	0.1	2
200	11	1	10	8648.1122	0.1	2
200	11	2	10	8646.9346	0.2	3
200	11	3	9	8811.3048		1
200	11	3	8	8933.4063	0.9	2
200	11	4	8	8951.6643		1
200	11	4	7	9015.2322	0.3	2
200	11	5	7	9093.1731	1.0	2
200	11	6	6	9234.9645	1.5	2
200	11	7	4	9399.5957		1
200	12	0	12	8678.9116	6.9	3
200	12	1	11	8885.9542		1
200	12	2	11	8886.8882	0.1	2
200	12	2	10	9068.2520		1
200	12	3	10	9067.4763	0.4	2
200	12	3	9	9213.3625		1
200	12	4	9	9221.2277	0.6	3
200	12	5	8	9351.3212	0.9	3
200	12	6	7	9517.9966		1
200	13	0	13	8917.3899	0.3	2
200	13	1	13	8917.3881	0.8	2
200	13	1	12	9143.3948	1.2	2
200	13	2	12	9143.4743	0.3	2
200	13	2	11	9343.5263		1
200	13	3	10	9508.8582		1
200	13	4	10	9512.7975		1
200	13	5	9	9659.4381		1
200	14	0	14	9173.1112		1
200	14	1	14	9173.1108		1
200	14	2	13	9417.2673		1
002	5	5	1	8099.3675		1
002	6	1	6	7849.7186	0.2	3
002	6	3	3	8053.4801	0.4	3
002	6	6	0	8377.5074		1
002	7	0	7	7983.6249	0.5	3
002	7	2	5	8177.4365	0.3	3
002	7	4	4	8298.4955	0.6	4
002	7	6	2	8547.2256	0.7	2
002	7	6	1	8547.2357	0.4	2
002	7	7	1	8699.1814		1
002	8	0	8	8136.4073	0.4	2
002	8	1	8	8135.6624	0.4	3
002	8	1	7	8268.9752		1
002	8	2	6	8370.2809	0.8	3
002	8	3	6	8386.9512	0.1	5
002	8	3	5	8436.4969	0.4	3
002	8	4	5	8489.3264	0.5	5
002	8	4	4	8502.6578	0.3	3
002	8	5	3	8606.0100	0.0	2
002	8	6	2	8740.4319		1
002	8	7	2	8886.7919	0.4	3
002	8	7	1	8886.7917	0.2	2
002	8	8	1	9062.5338		1
002	8	8	0	9062.5339		1
002	9	0	9	8305.5237		1
002	9	1	8	8457.6689		1
002	9	2	7	8579.8471	0.1	2
002	9	3	7	8585.6338	0.7	4
002	9	3	6	8663.4480	0.3	3
002	9	4	6	8702.2357	0.1	2
002	9	4	5	8727.8601		1
002	9	5	5	8820.6164	1.4	2
002	9	5	4	8824.7015	0.2	2
002	9	6	4	8956.9536	0.1	2
002	9	6	3	8957.2187	1.1	2
002	9	7	3	9099.7364		1
002	9	7	2	9099.7450	1.9	2
002	9	8	2	9282.6213	1.3	2
002	9	8	1	9282.6201	0.7	2
002	9	9	1	9465.8022		1
002	9	9	0	9465.8024		1
002	10	1	9	8661.8671	0.4	2

(*continued on next page*)

Table 2 (continued)

V	J	K_a	K_c	E	δ	N
002	10	2	9	8663.1332		1
002	10	2	8	8805.6056		1
002	10	3	8	8809.1498	0.1	3
002	10	3	7	8910.2117	1.5	2
002	10	4	7	8936.1951	0.4	3
002	10	4	6	8985.5192	0.6	3
002	10	5	6	9059.6286		1
002	10	5	5	9069.6435	0.5	2
002	10	6	5	9196.8772	0.3	2
002	10	6	4	9197.7808	0.2	2
002	10	7	4	9336.8057		1
002	10	8	3	9524.9394	0.8	2
002	10	8	2	9524.9366	1.8	2
002	10	9	2	9704.2642		1
002	10	9	1	9704.2645		1
002	11	0	11	8698.0205		1
002	11	1	11	8698.0176		1
002	11	1	10	8886.1325		1
002	11	2	10	8886.2835		1
002	11	2	9	9048.9379	0.8	2
002	11	3	9	9046.6338	0.5	3
002	11	3	8	9174.1735	1.1	2
002	11	4	8	9190.2742		1
002	11	4	7	9261.5969		1
002	11	5	7	9320.8893	1.0	2
002	11	5	6	9341.5378		1
002	11	6	6	9459.9111		1
002	11	6	5	9462.5050	0.0	2
002	11	8	4	9789.6716		1
002	11	8	3	9789.6646		1
002	12	0	12	8920.5690		1
002	12	1	12	8920.5630		1
002	12	1	11	9126.7376		1
002	12	2	11	9126.7953		1
002	12	3	10	9305.9547	2.0	2
002	12	4	9	9464.2246		1
002	12	5	8	9603.4713		1
002	12	6	7	9745.6650		1
002	13	0	13	9160.5607		1
002	13	1	13	9160.5578		1
002	13	1	12	9384.6221		1
002	13	2	12	9384.6225		1
002	13	4	10	9747.7662		1
040	1	1	1	6170.3255		1
040	4	2	2	6508.7345	1.3	3
040	4	4	0	6886.4243	2.1	2
040	5	2	4	6615.2305	3.6	2
040	5	3	2	6794.3724	1.1	3
040	5	5	1	7257.8709		1
040	5	5	0	7257.8765	1.6	4
040	6	0	6	6564.4767		1
040	6	2	4	6794.0341		1
040	6	4	3	7154.3338		1
040	6	4	2	7154.5229	0.8	2
040	6	6	1	7680.6785		1
040	7	1	7	6708.7352		1
040	7	2	6	6913.5746	0.3	2
040	7	2	5	6977.0338		1
040	7	3	5	7106.4507		1
040	7	3	4	7117.0564	0.0	2
040	7	4	4	7324.5194		1
040	7	6	2	7852.5875		1
040	7	6	1	7852.5881		1
040	8	2	7	7093.5607	1.6	2
040	8	3	6	7297.8731	0.9	2
040	8	4	5	7518.5472	9.2	2
040	8	5	4	7769.3690	1.0	2
040	8	7	2	8344.3723		1
040	9	1	8	7270.7650		1
040	9	6	4	8267.7876		1
040	9	7	2	8564.7827		1
040	10	3	8	7746.0151		1
040	11	5	7	8502.0104	2.0	2
040	12	1	12	7659.1572		1
040	12	3	10	8280.4377		1
040	12	6	6	9065.7337		1
040	13	6	7	9379.8680		1

They are then compared with the compilation given by [6]. The results of this comparison are shown in Table 1. Totally 290 new energy levels have been obtained for six upper vibrational states of the first hexad. The origin of the (040)–(000) band has been estimated to be $6110.41 \pm 0.01\ \mathrm{cm}^{-1}$ not only from the obs. – calc. tendency for the energy levels with $K_a = 0$ of the (040) state, but also from the fitting of the low K_a energy levels up to $J = 5$. Detailed comparison of our energy levels set with compilation [6] has shown that the levels from both sets agree within $0.0012\ \mathrm{cm}^{-1}$ on average. We did not confirm 18 energy levels derived in [3–5]. Full set of the obtained energy levels is presented in the electronic archive attached to the paper. New energy levels derived in this work are shown in Table 2, which contains also 41 levels which have been presented in [3–5], but our values differ from the literature data by more than $0.004\ \mathrm{cm}^{-1}$. We believe that our values are more reliable since they are derived from the combination differences of several lines or from stronger line compared to [3–5].

The resonance interactions between the first hexad states are similar to those accounted for in [11] for the first hexad of $H_2{}^{16}O$. Thus, the (040) state may be considered as being isolated up to $J \leqslant 4$. From $J = 5$, high K_a levels of the (040) state become to be perturbed due to the resonances connected with the (120), (021), and (101) states. This interaction induces considerable intensity transfer to corresponding transitions of the weak $4\nu_2$ band making them observable. Such a behavior is typical for highly excited bending state: first, the energy of its levels becomes comparable with that of other polyad members only for high J and K_a values; second, abnormal centrifugal distortion which accompanies excitation of the large amplitude bending vibration, strengthens the resonance. In our spectrum, we observe a number of very strong transitions of the $4\nu_2$ band involving $J = 7$–11, and $K_a = 4$–6 energy levels. Some of these transitions dominated all over the spectrum in the $4\nu_2$ band what is shown in Fig. 3. On the upper panel of this figure, an overview of the strong $\nu_2 + \nu_3$ band which is less distorted by resonance perturbations, is also presented for comparison.

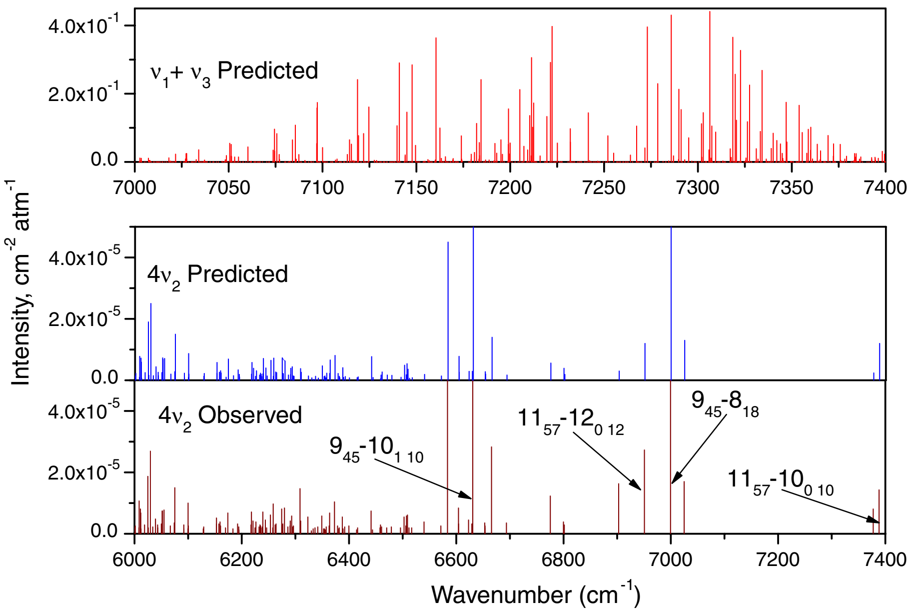

Fig. 3. Overview of the stick spectrum of the $4\nu_2$ and $\nu_2 + \nu_3$ bands of $H_2{}^{18}O$. Intensity scale corresponds to pure $H_2{}^{18}O$. Strong transitions in the high frequency end of the $4\nu_2$ band spectrum borrows their intensities through resonance interactions.

4. Conclusion

FT spectrum of the $H_2{}^{18}O$ molecule was recorded and assigned in the 6000–7940 cm^{-1} spectral region based on the high accuracy Partridge and Schwenke [7,8] calculations. Detailed $H_2{}^{18}O$ absorption list was generated and verified in the considered spectral region. A set of 290 new accurate energy levels for six vibrational states of the first hexad was derived. The results obtained may be useful both for atmospheric applications and refining the potential energy surface of the water molecule.

Acknowledgments

This work was jointly supported by the Natural Science Foundation of China (20473079 and 10574124), the Chinese Academy of Science and by the INTAS foundation (project 03-51-3394). This work also forms part of an effort by a Task Group of the International Union of Pure and Applied Chemistry (IUPAC, Project no. 2004-035-1-100). B. Voronin acknowledges the financial support from EC program FP6, Marie Courie Incoming Fellowships, Grant WWLC008535. O. Naumenko also thanks for guest professorship supported by the Foundation for Educational Development and Research of USTC-SIAS.

Appendix A. Supplementary material

Supplementary data for this article are available on ScienceDirect (www.sciencedirect.com) and as part of the Ohio State University Molecular Spectroscopy Archives (http://msa.lib.ohio-state.edu/jmsa_hp.htm).

References

[1] J.-P. Chevillard, J.-Y. Mandin, C. Camy-Peyret, J.-M. Flaud, Can. J. Phys. 64 (1986) 746–761.
[2] R.A. Toth, Appl. Opt. 33 (1994) 4868–4879.
[3] P. Macko, D. Romanini, S.N. Mikhailenko, O.V. Naumenko, S. Kassi, A. Jenouvrier, Vl.G. Tyuterev, A. Campargue, J. Mol. Spectrosc. 227 (2004) 90–108.
[4] R.N. Tolchenov, J. Tennyson, J. Mol. Spectrosc. 231 (2005) 23–27.
[5] R.A. Toth, J. Quant. Spectrosc. Radiat. Transf. 94 (2005) 51–107. http://mark4sun.jpl.nasa.gov .
[6] S. Mikhailenko, S. Tashkun, private communication.
[7] H. Partridge, D.W. Schwenke, J. Chem. Phys. 106 (1997) 4618–4639.
[8] D.W. Schwenke, H. Partridge, J. Chem. Phys. 113 (2000) 6592–6597.
[9] L.S. Rothman, D. Jacquemart, A. Barbe, D. Chris Benner, M. Birk, L.R. Brown, M.R. Carleer, C. Chackerian Jr, K. Chance, V. Dana, V.M. Devi, J.-M. Flaud, R.R. Gamache, A. Goldman, J.-M. Hartmann, K.W. Jucks, A.G. Maki, J.Y. Mandin, S.T. Massie, J. Orphal, A. Perrin, C.P. Rinsland, M.A.H. Smith, J. Tennyson, R.N. Tolchenov, R.A. Toth, J. Vander Auwera, P. Varanasi, G. Wagner, J. Quant. Spectrosc. Radiat. Transfer. 96 (2005) 139–204.
[10] S.N. Mikhailenko, Vl.G. Tyuterev, G. Mellau, J. Mol. Spectrosc. 217 (2003) 195–211.
[11] A. Bykov, O. Naumenko, A. Scherbakov, L. Sinitsa, Atmos. Oceanic Opt. 17 (2004) 940–947.